Aperture alteration pattern in silicate and carbonate reservoirs during cold water injection and heat extraction

Abhijit Chaudhuri and Sachchida Nand Pandey
Indian Institute of Technology Madras, Chennai-36, Tamil Nadu, India

Introduction

In an Enhanced Geothermal System (EGS) the heat energy is usually extracted from deep reservoir by circulating water (cold water is injected and hot water is pumped). The fractures/joints in geothermal reservoir play a significant role because they are the main flow conduits where permeability of the rock matrix is very low. Sometime a single fracture or fault extends very long can connect the injection and production wells [Rawal and Ghassemi, 2014; Pandey et al. 2014 and 2015]. The transmissivity of fracture is sensitive to fracture aperture and spatial heterogeneity in aperture field. During the EGS operation the aperture is subjected to alteration due to dissolution/precipitation of reservoir minerals during. The transmissivity alteration greatly influences the flow impedance and temperature drawdown at production well depending on the type of minerals, range of temperature and injection conditions. So the study of hydrologic evolution of EGS is very important for planning of sustainable energy recovery [Mroczek et al., 2000; Rabemanana et al., 2003 Bachler and Kohl, 2005].

We simulated the hydrologic evolution of EGS for two types of rocks which very are common in earth's formation namely carbonate and silicate. For the numeral experiment we assumed that carbonate rock was only made of calcite ($CaCO_3$) and in silicate reservoir silica was present as amorphous silica (SiO_2). We selected these minerals because these are more reactive than others and calcite is retrograde soluble while amorphous silica is prograde soluble (see Fig. 1). Figure (1) also shows that reaction rate increases with temperature for both calcite and amorphous silica. We also simulated for heterogeneous aperture field and compared the effect of heterogeneity on the evolution of reservoirs of two types of minerals.

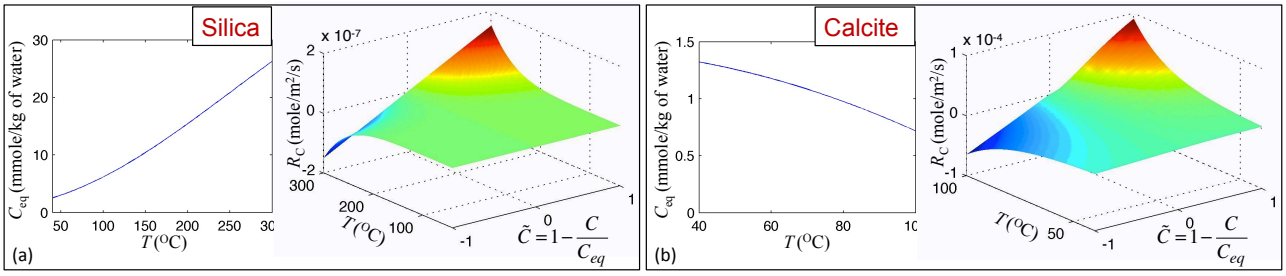

***Figure** 1: Temperature dependent solubility and reaction kinetics of (a) amorphous silica and (b) calcite.*

Mathematical Modeling

The following aperture integrated mass momentum and energy balance equations are used to model flow, heat transfer and solute transport through a single fracture [Ortoleva et al., 1987; Chaudhuri et al., 2013]:

$$\nabla.\mathbf{Q} = f_Q \ , \qquad \mathbf{Q} = -\frac{b^3}{12\mu F_T}\left(\nabla P + \rho \mathbf{g}\right), \tag{1}$$

$$\frac{\partial\left(b\rho c_p T\right)}{\partial t} + \mathbf{Q}.\nabla h - b\nabla.\left(\lambda \nabla T\right) = f_T \ \text{ and } \ \frac{\partial\left(b\rho C\right)}{\partial t} + \mathbf{Q}_f.\nabla\left(\rho C\right) - b\nabla.\left(D\nabla\left(\rho C\right)\right) = R_C + f_C \,,$$

where b, $\mathbf{Q}$, P, T, and C are fracture aperture, aperture integrated flux vector, aperture averaged pressure, temperature and concentration respectively. The flow, transport of heat and solute within low permeable porous medium are governed by general 3-D Darcy and advection-dispersion equations respectively for porous medium. In Eq. (1) f_Q, f_T, and f_C are respectively fluid, heat and solute exchange between rock matrix and fracture. The expressions of these terms are available in [Pandey et al. 2014]. In the solute transport equations (Eq. 1), R_C denotes the reaction due to mineral dissolution and precipitation. The simplified form of reaction rate for amorphous silica and calcite were derived based on the consideration of equilibrium of aqueous phase ions. For silica the formulation of R_C is simpler and it can be expressed as a function of temperature and saturation index, $\tilde{C} = 1 - C/C_{eq}$ [Rimstidt and Barnes, 1980]. For calcite due to multiple chemical reactions among various ions, the formulation of R_C is significantly complicated. Plummer et al. [1978] provided an implicit formula for R_C in terms of concentration of ions. Later Chaudhuri et al. [2013] used Tableaux method and fitted polynomials to express R_C in terms of temperature and saturation index. Figure (1) shows the variations of C_{eq} and R_C with temperature for amorphous silica and calcite.

The aperture alteration rate: $\frac{\partial b}{\partial t} = \frac{R_C}{\rho_r \omega}$, where $\rho_r \omega$ is the mole of mineral per unit volume of rock.

Results and discussions

From the Fig. (1) it is very clear that the reaction rate for calcite is a few orders of magnitude higher than amorphous silica. So the evolution of aperture alteration should be significantly faster in carbonate reservoir than silicate reservoir. In addition to this the retrograde soluble calcite is expected to cause remarkable difference in the pattern of evolution in comparison to that caused by prograde soluble amorphous silica. For a quantitative comparison of the pattern formation inside the fracture, one must simulate for same setup. However we feel that a qualitative comparison is more insightful for evolution of EGS, which is located in either silicate or carbonate reservoirs. We considered different temperature range and initial aperture of the fracture in silicate and carbonate reservoirs such that enough hydrological alterations took place in life span of a EGS. Schematic of a reservoir that consists of a horizontal fracture is shown in Fig. (2). The temperature range, initial aperture and injection conditions for silicate and carbonate reservoirs are given in Table 1. Aperture alterations (Δb), corresponding temperature (T) and aperture-integrate flux vector ($\mathbf{Q}$) for silicate and carbonate reservoirs are shown in Figs. (3) and (5) respectively.

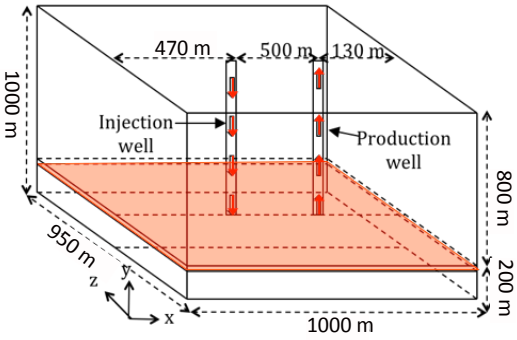

Figure 2: *Schematic diagram*

Table 1: *Initial aperture field, temperature range and injection conditions for silicate and carbonate reservoir.*

Reservoir	T_{frac} (^{O}C) & $\frac{dT}{dz}$ (^{O}C/km)	b_{ini} (mm)	T_{inj} (^{O}C)	C_{inj} (mmole/kg)
Silicate	260 & 200	0.5	160	0 & 22
Carbonate	84 & 80	1	20	1.033 & 1.1

To evaluate the impact of injection temperature and concentration, we considered two different injection conditions as indicated in Table 1. To simulate the maximum influence resulting from the injected water, we considered two extreme cases: (i) fresh water injection, i.e. $C_{inj} = 0$ and (ii) C_{inj} equal to C_{eq} amorphous silica at the initial fracture temperature, 260 ^{O}C. In second case the injected water is oversaturated. Figure (3a1) shows that the fresh water injection causes dissolution of rock and growth of aperture. However the growth is very large in the outer region. It is because the temperature, which is higher in outer region (see Fig. 3b1), is the controlling

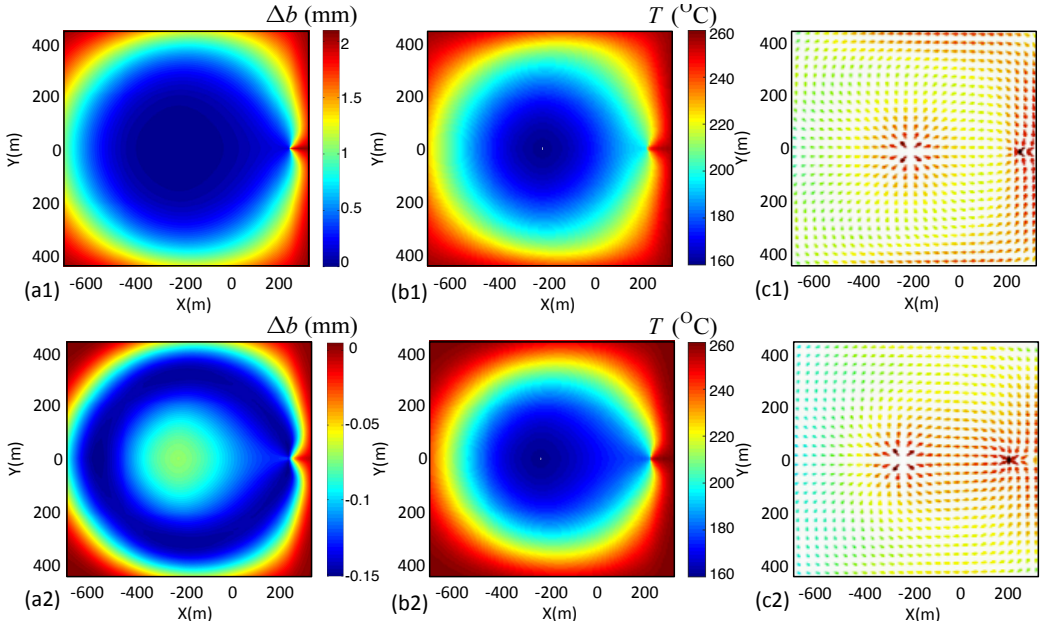

Figure 3*: Aperture alteration, evolution of temperature and flow fields after* 20 *years of operation in silicate reservoir for (a1,b1,c1) dissolution case,* $C_{inj} = 0$ *and (a2,b2,c2) precipitation case,* $C_{inj} = 22$ *mmole/kg.*

factor than saturation index in determining the magnitude of reaction rate. See Section 4.1 and Fig. 7 in [Pandey et al., 2015] for detail explanation. In this case water travel more in the outer region as shown in Fig. (3c1). It helps to bring more heat energy to the production well. The drawdown of production temperature (T_{pro}) and pressure difference ($\Delta P = P_{inj} - P_{pro}$) are shown respectively in Figs. (6b1) and (6c1). For the case of dissolution T_{pro} decreases slower than nonreactive case and the injection pressure decreases steadily with time. Figure (3a2) shows that oversaturated water injection ($C_{inj} = 22$ mmole/kg) causes precipitation. However significant aperture reduction takes place at some distance away from the injection well along a band (indicated by blue color in Fig. 3a2). Water does not flow much in the outer region due to the formation of low aperture band. Figures (3b2 and

3c2) show that the cooling and flow happen over a smaller area in case precipitation than dissolution. Figure (6b2) shows that for precipitation case T_{pro} decreases at same rate of nonreactive case. Because of aperture reduction, ΔP increases with time as seen in Fig. (6c2).

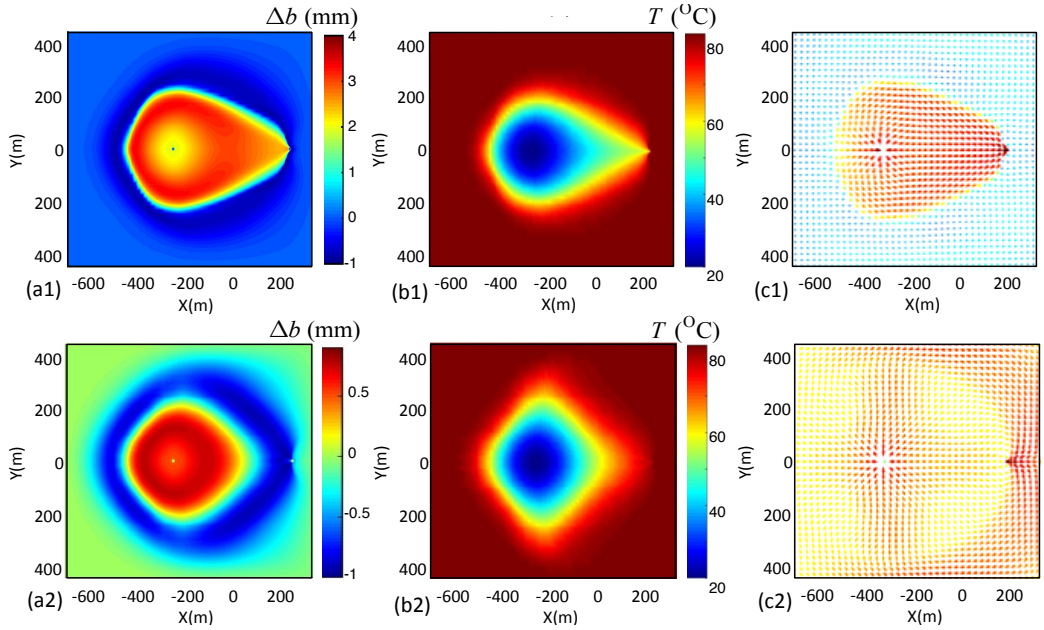

Figure 4: *Aperture alteration, evolution of temperature and flow in carbonate reservoir for (a1,b1,c1) dissolution case, C_{inj} = 1.033 mmole/kg after 500 days and (a2,b2,c2) precipitation case, C_{inj} = 1.1 mmole/kg after 150 days.*

To demonstrate the effect reactive aperture alteration in carbonate rock we considered the injections conditions as given in Table 1. Similar to silica, we also considered the first case as $C_{inj} = C_{eq}$ at initial fracture temperature. At T =84 ^{O}C, C_{eq} =1.033 mmole/kg of water. Thus for retrograde soluble calcite, the injected water (T_{inj} = 20 ^{O}C) is undersaturated. Figure (4a1) shows very large growth of aperture around the injection well within 500 days of operation. However a low aperture band (in dark blue) outside the high aperture zone is also formed (as seen in Fig. 5a1). It plays an important role modifying the flow field. Figure (4c1) shows that significantly small amount of fluid flows past the low permeability and injected water mostly gets channelized through the high aperture zone to production well. As a result the cooling is restricted to the oval-shaped dissolution zone (see Fig. 4b1). Figures (7b1) and (7c1) show rapid drop of T_{pro} and ΔP respectively. A non-monotonic decrease of ΔP is seen for the case of dissolution in carbonate reservoir. Since $C_{inj} = C_{eq}$ at T =84 ^{O}C caused very rapid dissolution and aperture growth, we were to curious to see the effect of slight increase of C_{inj} in second case.Figures (4a2 - 4c2) shows that the overall results for C_{inj} =1.1 mmole/kg are completely different from the case of C_{inj} =1.033 mmole/kg even though dissolution and precipitation take place simultaneously for both cases. For C_{inj} =1.1 mmole/kg, the precipitation seems to be dominant and a low permeable barrier is formed before the production well (see Fig. 4a2). The flow field and cooling are also modified accordingly (see Fig. 4b2 and 4c2). In this case effective transmissivity decreases very fast and Fig. (7c2) shows that ΔP grows three times within 150 days. However the decrease of T_{pro} is insignificant (see Fig. 7b2).

We also studied the effect of heterogeneous distribution of initial aperture on the dissolution/precipitation patter formation. We considered lognormal distribution of initial aperture and exponential spatial correlations. A representative initial heterogeneous aperture field is shown in Fig. (5). This was generated for $\sigma_{\ln b} = 0.5$ and correlation lengths, $\lambda_x = \lambda_y = 15$ m. The growth and reduction of aperture for four cases (Silica: C_{inj} =0 and 0.022 mole/kg and Calcite: C_{inj} =1.033 and 1.1 mmole/kg) are shown in Figs. (6a1, 6a2, 7a1 and 7a2) respectively. In Figs. (6 and 7) T_{pro} vs t and ΔP vs t curves for various initial aperture fields are shown to compare with respective homogeneous cases. The dash-dot lines are for $\lambda_x = \lambda_y = 15$ m and dash lines are for $\lambda_x = \lambda_y = 45$ m. The irregularities in the shapes of the color contours are very clear in Figs. (6a1, 6a2, 7a1 and 7a2). For smaller correlation lengths T_{pro} and ΔP are affected very less for silicate reservoir (see Fig. 6) but some notable differences can be seen in Fig. (7) for carbonate reservoir. Heterogeneity affects more when the correlation lengths are large. For dissolution case in carbonate reservoir, the shapes of the curves are different. However the significant effect is seen for C_{inj} = 1.1 mmole/kg in carbonate reservoir. In some cases ΔP does not increase rapidly rather shows a trend of decrease with time.

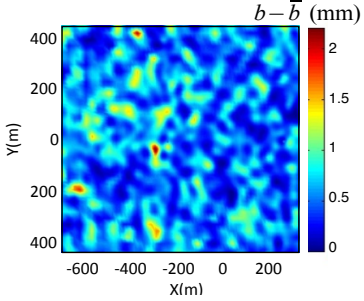

Figure 4: *A representative sample of heterogeneous aperture field.*

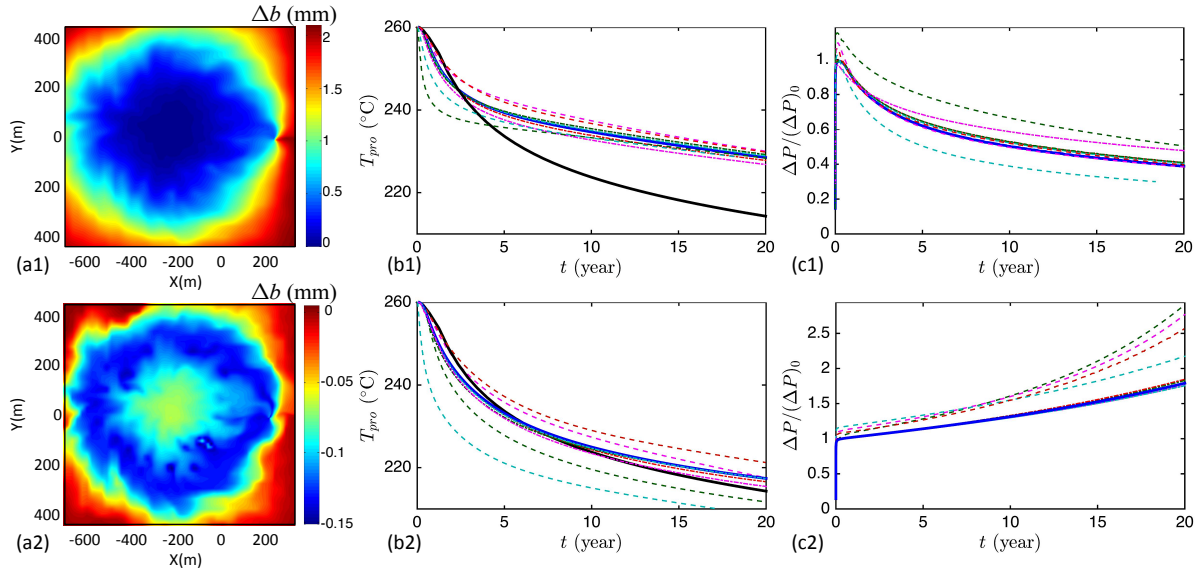

Figure 6: *Effects of initial heterogeneous aperture on* Δb *,* T_{pro} vs t *and* ΔP vs t *curves for silicate reservoir: (a1,b1,c1) dissolution case* $C_{inj} = 0$ *and (a2,b2,c2) precipitation case* $C_{inj} = 22$ *mmole/kg.*

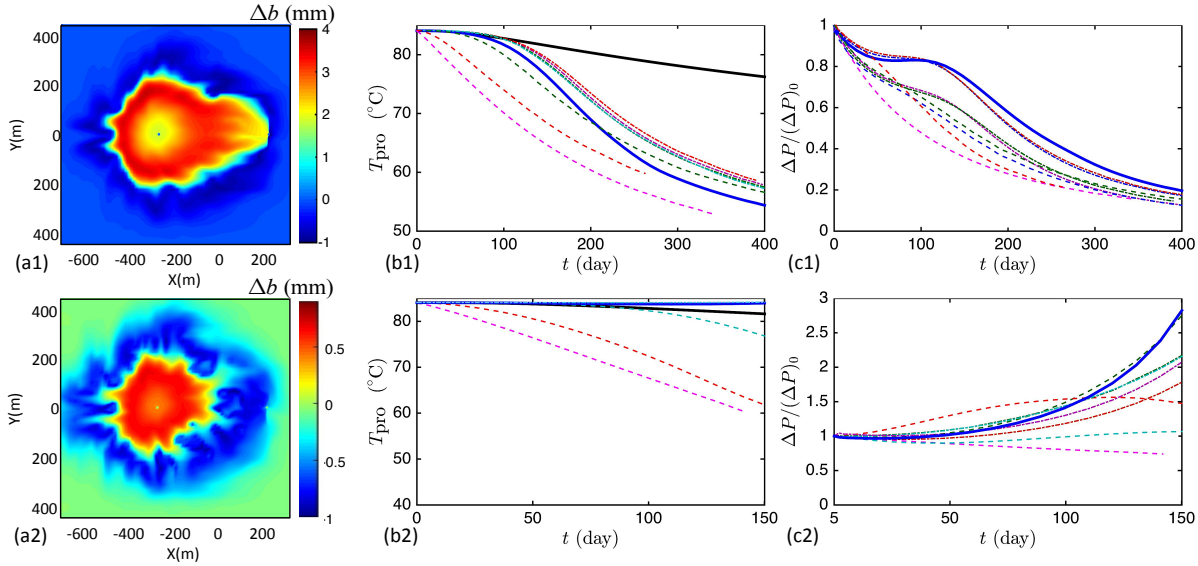

Figure 7: *Effects of initial heterogeneous aperture on* Δb *,* T_{pro} vs t *and* ΔP vs t *curves for carbonate reservoir: (a1,b1,c1) dissolution case* C_{inj} =1.033 mmole/kg *and (a2,b2,c2) precipitation case* C_{inj} =1.1 *mmole/kg.*

Summary: Very fast reaction rate and retrograde solubility of calcite resulted in very contrasting dissolution/precipitation pattern carbonate reservoir when compared with silicate reservoir. The effects of heterogeneity are also more prominent in carbonate reservoir.

References

1. Chaudhuri, A., Rajaram, H., Viswanathan, H., 2008. Alteration of fractures by precipitation and dissolution in gradient reaction environments: computational results and stochastic analysis. Water Resource Research 44, W10410, http://dx.doi.org/10.1029/2008WR006982.
2. Pandey, S.N., Chaudhuri, A., Kelkar, S., Sandeep, V.R., Rajaram, H., 2014. Investigation of permeability alteration of fractured limestone reservoir due to geothermal heat extraction using three-dimensional thermo-hydro-chemical (THC) model. Geothermics 51, 46– 62.
3. Pandey, S.N., Chaudhuri, A., Rajaram, H, Kelkar, S.,Fracture transmissivity evolution due to silicadissolution/precipitation during geothermal heat extraction, Geothermics, 578, 111 – 126, 2015.
4. Rawal, C., Ghassemi, A., 2014. A reactive thermo poroelastic analysis of water injection into an enhanced geothermal reservoir. Geothermics 50, 10–23.
5. Rimstidt, J.D., Barnes, H.L., 1980. The kinetics of silica–water reactions. Geochim. Cosmochim. Acta 44, 1683–1699.
6. Mroczek, E.K, White, S.P, Graham, D.J., 2000. Deposition of amorphous silica in porous packed beds - predicting the lifetime of reinjection aquifers. Geothermics 29, 737-757.
7. Plummer L.N., T.M.L. Wigley, D.L. Parkhurst, 1978, The kinetics of calcite dissolution in CO_2–water systems at 5° and 60 °C and 0.0 to 1.0 atm. CO_2, Am. J. Sci., 278, 179–216.
8. Rabemanana V, Durst P., Bachler D., Vuataz F.and Kohl T., 2003. Geochemical modeling of the Soultz-sous-Forets Hot Fractured Rock system comparison of two reservoirs at 3.8and 5 km depth, Geothermics 32, 645–653.
9. Bachler, D, Kohl T, 2005. Coupled thermal-hydraulic-chemical modeling of enhanced geothermal systems, Geophys. J. Int. 161 (2), 533–548